Probing Hydrogen-Bonding Interactions in the Active Site of Medium-Chain Acyl-CoA Dehydrogenase Using Raman Spectroscopy†

Jiaquan Wu,‡ Alasdair F. Bell,‡ Lian Luo,§ Avery W. Stephens,§ Marian T. Stankovich,§ and Peter J. Tonge*,‡

Department of Chemistry, State University of New York at Stony Brook, Stony Brook, New York 11794-3400, and Department of Chemistry, University of Minnesota, Minneapolis, Minnesota 55455-0431

Received March 20, 2003; Revised Manuscript Received June 18, 2003

ABSTRACT: The role of the oxyanion hole in the reaction catalyzed by pig medium-chain acyl-CoA dehydrogenase (pMCAD) has been investigated using enzyme reconstituted with 2′-deoxy-FAD. The k_{cat} (18.8 ± 0.5 s^{-1}) and K_m (2.5 ± 0.4 μM) values for the oxidation of *n*-octanoyl-CoA (C_8-CoA) by WT pMCAD recombinantly expressed in *Escherichia coli* are similar to those of native pMCAD isolated from pig kidney. In agreement with previous studies [Engst et al. (1999) *Biochemistry 38*, 257−267], reconstitution of the WT enzyme with 2′-deoxy-FAD causes a large (400-fold) decrease in k_{cat} but has little effect on K_m. To investigate the molecular basis for the alterations in activity resulting from changes in hydrogen bonding between the substrate and the enzyme's oxyanion hole, the structure of the product analogue hexadienoyl-CoA (HD-CoA) bound to the 2′-deoxy-FAD-reconstituted enzyme has been probed by Raman spectroscopy. Importantly, while WT pMCAD causes a 27 cm^{-1} decrease in the vibrational frequency of the HD enone band, from 1595 to 1568 cm^{-1}, the enone band is only shifted 10 cm^{-1} upon binding HD-CoA to 2′-deoxy-FAD pMCAD. Thus, removal of the 2′-ribityl hydroxyl group results in a substantial reduction in the ability of the enzyme to polarize the ground state of the ES complex. On the basis of an analysis of a similar system, it is estimated that ground state destabilization is reduced by up to 17 kJ mol^{-1}, while the activation energy for the reaction is raised 15 kJ mol^{-1}. In addition, removal of the 2′-ribityl hydroxyl reduces the redox potential shift that is induced by HD-CoA binding from 18 to 11 kJ mol^{-1}. Consequently, while ligand polarization caused by hydrogen bonding in the oxyanion hole is intimately linked to substrate turnover, additional factors must be responsible for ligand-induced changes in redox potential. Finally, while replacement of the catalytic base E376 with Gln abolishes the ability of the enzyme to catalyze substrate oxidation and to catalyze the exchange of the C_8-CoA α-protons with solvent deuterium, the 2′-deoxy-FAD-reconstituted enzyme catalyzes α-proton exchange at a rate (k_{exc}) of 0.085 s^{-1}, which is only 4-fold slower than k_{exc} for WT pMCAD (0.35 s^{-1}). Thus, either the oxyanion hole plays only a minor role in stabilizing the transition state for α-proton exchange, in contrast to its role in substrate oxidation, or the value of k_{exc} for WT pMCAD reflects a process such as exchange of the E376 COOH proton with solvent.

Mammalian acyl-CoA dehydrogenases (ACDs) catalyze the first step in the fatty acid β-oxidation pathway in which fatty acyl-CoAs are oxidized to the corresponding *trans*-2-enoyl-CoAs (*1*, *2*). Mechanistic studies on the medium-chain enzyme (MCAD)[1] have established that substrate oxidation occurs via abstraction of the substrate's *pro-2R* proton by a general base (E376) with the concurrent transfer of the *pro-3R* hydrogen as a hydride to the FAD cofactor (Scheme 1). This reaction presents two thermodynamic challenges. First, the pK_a of a typical glutamate residue is around 5, while

Scheme 1

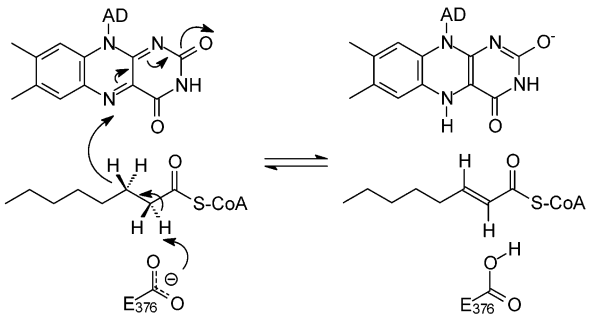

those of the α-protons of the free fatty acyl-CoA substrate are around 21 (*3*). Second, the midpoint potential (E_m) of FAD in free pig MCAD is −145 mV vs standard hydrogen electrode (SHE) while that of the octanoyl-CoA/octenoyl-CoA couple is −38 mV (*4*), thereby hindering electron transfer from substrate to cofactor. Both of these barriers to substrate oxidation are overcome by changes in pK_a and redox potential that accompany ligand binding, and our

† This work was supported by NIH Grants GM63121 (P.J.T.) and GM29344 (M.T.S.). P.J.T. is an Alfred P. Sloan Research Fellow. In addition, this material is based upon work supported in part by the U.S. Army Research Office under Grant DAAG55-97-1-0083.

* To whom correspondence should be addressed. Telephone: (631) 632-7907. Fax: (631) 632-7960. E-mail: peter.tonge@sunysb.edu.

‡ SUNY at Stony Brook.

§ University of Minnesota.

[1] Abbreviations: MCAD, medium-chain acyl-CoA dehydrogenase; CoA, coenzyme A (lithium salt); C_8-CoA, *n*-octanoyl-CoA; HD-CoA, hexadienoyl-CoA; 2′-deoxy-FAD pMCAD, pig MCAD reconstituted with 2′-deoxy-FAD.

10.1021/bi0344578 CCC: $25.00
Published on Web 09/18/2003

interest centers on understanding the molecular details of this process.

On the basis of pH dependence studies, Ghisla et al. concluded that the pK_a of E376 in human MCAD was raised to 7.9 upon binding hexanoyl-CoA (*5*). In addition, Vock and co-workers used a spectrophotometric method to determine that the α-proton pK_a of *p*-NO_2-phenylacetyl-CoA (4NPA-CoA) was reduced from 13.6 to 5 upon binding to human MCAD (*6*). Correspondingly, the α-proton pK_a of (3*S*)-C_8-CoA was lowered from 16.5 to 5.2 upon binding to enzyme (*6*). The trends observed in these analogues suggested that the pK_a shifts of normal substrates such as *n*-octanoyl-CoA (C_8-CoA) would be even higher considering the optimal structural compatibility between the substrate and the enzyme's active site (*5*−*7*). Consequently, to minimize the barrier to substrate deprotonation, the pK_a of E376 is raised upon substrate binding while the pK_as of the substrate's α-protons are lowered. In addition to the pK_a changes, substrate binding also modulates the redox potential, and Lenn et al. demonstrated that the E_m of pig MCAD shifted positive by over 120 mV upon binding substrate, thus facilitating electron transfer from substrate to enzyme (*4*).

The crystal structure of pig MCAD complexed with C_8-CoA revealed that the carbonyl oxygen of the substrate is within hydrogen-bonding distance of both the 2′-hydroxyl group of the FAD cofactor (2.9 Å) and the backbone amide of E376 (3.1 Å) (*8*). These hydrogen-bonding interactions, strongly reminiscent of the oxyanion hole first described in proteases (*9*), may play an essential role in substrate polarization and catalysis (*10*, *11*). The importance of the ribityl hydrogen bond in catalysis was demonstrated by Engst et al., who used enzyme reconstituted with 2′-deoxy-FAD to show that removal of the 2′-ribityl hydrogen bond donor resulted in a 1.5×10^7-fold reduction in k_2, a kinetic parameter determined by monitoring the bleaching of the flavin absorption (*11*). In addition, removal of the 2′-ribityl hydrogen bond was also found to reduce the midpoint potential change observed on ligand binding. Johnson et al. observed that the flavin E_m of the 2′-deoxy-FAD pMCAD was shifted positive by only 30 mV upon binding the substrate analogue 2-azaoctanoyl-CoA. This 30 mV positive shift represents only 40% of the midpoint potential shift observed with native MCAD upon binding the same analogue (*12*).

Previously, we reported experimental evidence of product analogue polarization by pig MCAD (pMCAD) on the basis of electrochemical and Raman spectroscopic studies (*13*). The electronic structure of a product analogue, hexadienoyl-CoA (HD-CoA), was altered upon binding to both the oxidized and the reduced forms of the enzyme, as shown by changes in the Raman spectrum of the analogue upon binding to the enzyme. Specifically, it was shown that the vibrational band arising from the C3═C2−C1═O enone portion of the analogue decreased 30 cm^{-1} upon binding to the enzyme. We believe that these changes in ligand structure reflect catalytically relevant interactions in the enzyme−product complex, and our interest is in determining the relationship between the observed polarization and the alterations in pK_a and E_m that accompany ligand binding.

To understand the relationship between hydrogen bonding, substrate polarization, and enzyme reactivity, we have used Raman spectroscopy to probe the electronic structure of HD-CoA bound to 2′-deoxy-FAD pMCAD, in which one of the hydrogen bond donors in the oxyanion hole has been deleted. The effect of this mutation on the rate of substrate oxidation and on the ability of the enzyme to catalyze the exchange of the C_8-CoA α-protons with solvent deuterium has been determined. In addition, we have also examined the consequence of removing the ribose hydroxyl group on the redox potential of the free enzyme and a complex with HD-CoA. These studies demonstrate that while ligand polarization and reactivity are intimately coupled, the polarization of the ligand that occurs on binding to the enzyme is not sufficient to account for the entire change in redox potential induced by ligand binding.

EXPERIMENTAL PROCEDURES

Chemicals. Hexadienoic acid, 1,1′-carbonyldiimidazole, acetaldehyde, [1-^{13}C]acetyl chloride, ferricenium hexafluorophosphate, and activated charcoal were from Aldrich while coenzyme A (lithium salt; CoA) was purchased from Sigma Chemical Co. [1,3-$^{13}C_2$]Malonic acid (99% ^{13}C), [2-^{13}C]-malonic acid (99% ^{13}C), and $H_2{}^{18}O$ (95−98% ^{18}O) were purchased from Cambridge Isotope Labs. Restriction endonucleases were purchased from New England Biolabs. T4 DNA ligase, *pfu* polymerase, *Escherichia coli* XL1 Blue supercompetent cells, and BL21(DE3) CodonPlus RIL(+) cells were obtained from Stratagene (La Jolla, CA). Primers were from Integrated DNA Technologies, Inc. (Coralville, IA).

Hexadienoyl-CoA and Isotope Labeling. Syntheses of hexadienoyl-CoA (HD-CoA) and isotope-labeled HD-CoAs have previously been described (*14*).

Synthesis and Characterization of n-Octanoyl-CoA (C_8-CoA). C_8-CoA was synthesized using the mixed anhydride method (*15*). ^{1}H NMR (600 MHz, D_2O): δ 0.78 (s, 3H, 11′ CH3), 0.87 (t, 3H, H8oct), 0.92 (s, 3H, 10′ CH3), 1.27 (m, 8H, H4−H7oct), 1.61 (quintuplet, 2H, H3oct), 2.47 (t, 2H, H6″), 2.62 (t, 2H, H2oct), 3.05 (t, 2H, H9″), 3.37 (t, 2H, H8″), 3.46 (t, 2H, H5″), 3.58 (q, 1H, H1″B), 3.86 (q, 1H, H1″A), 4.04 (s, 1H, H3″), 4.25 (s, 2H, H5′), 4.60 (s, 1H, H4′), 6.15 (d, 1H, H1′), 8.24 (s, 1H, H2), 8.54 (s, 1H, H8). The CoA H2′ and H3′ resonances are obscured by the solvent resonance.

Cloning of the pMCAD Gene into pET20b(+). A pMCAD cDNA clone was provided in a ZAP vector. Before amplification of the *pMCAD* cDNA, the internal *Nde*I restriction site was removed by QuikChange mutagenesis (Stratagene) using the primers MCAD4, 5′-GCA AAG GCA TAC GCT GCA GAT ATT GC-3′, and MCAD5, 5′-GC AAT ATC TGC AGC GTA TGC CTT TGC-3′. Subsequently, two primers were used to amplify the *pMCAD* gene and insert an N-terminal *Nde*I restriction site (MCAD2: 5′-CCT GGC AT**C ATA TG**G CAA AAG CTG TCC CAC AGT GTG-3′) and a C-terminal *Xho*I restriction site (MCAD3: 5′-CAT ATA GTG **CTC GAG** TTA ATT TTT ATA CCG GCC AAT GTG-3′). Since the first 25 amino acids of pig mitochondrial MCAD form the transit peptide, the amplification of the gene started from the codon for the 26th amino acid, lysine. The PCR product was digested, ligated into the pET20b(+) vector, and transformed into *E. coli* XL1 Blue cells (Stratagene). Finally, the stop codon at the C-terminus of the pMCAD gene was removed to enable expression of

the C-terminal His tag using the primers MCAD8, 5′-CGG TAT AAA AAT **CAA** CTC GAG CAC C-3′, and MCAD9, 5′-GGT GCT CGA G**TT G**AT TTT TAT ACC G-3′. All constructs were sequenced using the ABI sequencing method (Applied Biosystems).

Active Site Mutants. The E376Q and E376P mutants of pMCAD were generated by QuikChange mutagenesis using the primers MCAD10, 5′-CAG ATT TAT **CAA** GGT ACA GC-3′, and MCAD11, 5′-GCT GTA CC**T TG**A TAA ATC TG-3′, for E376Q and the primers MCAD12, 5′-CTA TCA GAT TTA T**CC A**GG TAC AGC ACA A-3′, and MCAD13, 5′-TTG TGC TGT ACC **TGG** ATA AAT CTG ATA G-3′, for E376P. The resulting plasmids were purified from XL1 Blue cells, and mutagenesis was confirmed by ABI sequencing.

Overexpression and Purification of Wild-Type and Mutant pMCAD Enzymes. Enzymes were expressed using BL21-(DE3) CodonPlus RIL(+) cells. Transformed cells were cultured to an OD_{600} of 1.0 in 1 L of rich media at 37 °C followed by protein expression at 28 °C using 1 mM IPTG (*16*). After overnight incubation, cells were harvested by centrifugation, resuspended in 200 mL of His-tag binding buffer (5 mM imidazole, 500 mM NaCl, 20 mM Tris, pH 8.7), and lysed by five passes through a French press cell. Following centrifugation for 90 min at 15000*g*, the supernatant was loaded onto a column (2.5 cm i.d.) packed with 10 mL of His-Bind resin (Novagen) and washed with 250 mL of binding buffer. Subsequently, protein was eluted by running a gradient of 5 mM to 1 M imidazole in the same buffer over 6 h at the flow rate of 2 mL/min. Green-yellow fractions containing MCAD protein were eluted at about 200 mM imidazole. Subsequently, the enzyme was degreened by adding solid sodium dithionite particles to the concentrated MCAD solution until the solution turned colorless. The enzyme solution was then loaded immediately onto a 30 × 1 cm Sephadex G-25 column equilibrated with 50 mM potassium phosphate and 0.3 mM EDTA, pH 7.6, to remove low molecular weight components.

General Methods. Recombinant pMCAD enzymes were concentrated using a Centricon-10 (Amicon), and the concentration of the oxidized enzymes was determined spectrophotometrically using an extinction coefficient of 15.4 mM^{-1} cm^{-1} at 446 nm (*17*). C_8-CoA was quantified using an extinction coefficient of 16.3 mM^{-1} cm^{-1} at 260 nm while HD-CoA was quantified using an extinction coefficient of 19.5 mM^{-1} cm^{-1} at 260 nm (*18*). Spectrophotometric experiments were performed on a Cary UV−vis spectrophotometer at 25 °C. *n*-Octynoyl-CoA was synthesized using the mixed anhydride method (*15*) and quantified using an extinction coefficient of 16.3 mM^{-1} cm^{-1} at 260 nm.

Reconstitution of Recombinant pMCAD with 2′-Deoxy-FAD. The FAD in recombinant pMCAD was replaced by 2′-deoxy-FAD using the reconstitution method of Mayer et al. (*19*). Specifically, 200 mg of Norit activated carbon was washed twice with 25 mL of 4 °C resolution buffer comprised of saturated $(NH_4)_2SO_4$ mixed with 3 M KBr in 6:1 volume ratio with 1 mM EDTA, pH 2.0, and subsequently resuspended in 40 mL of resolution buffer. A 15 mL NALGENE polycarbonate centrifuge tube containing 8 mL of the resolution suspension was precooled to ca. −5 °C in an ice−salt bath, and 0.8 mL of 180 μM pMCAD in 50 mM potassium phosphate and 0.3 mM EDTA, pH 7.6, buffer was added while the tube was swirled on a Vortex mixer gently for about 1 min. The suspension was then immediately centrifuged at 28000*g* (15000 rpm, Sorvall SS-34 rotor, 4 °C) for 5 min. Subsequently, the black pellet was resuspended by gentle swirling in 4 mL of 50 mM potassium phosphate buffer and 0.3 mM EDTA, pH 7.6 at 4 °C. The centrifugation step was repeated, and subsequently the supernatant was removed and assayed. The residual activity of native pMCAD was eliminated by incubating the apoprotein solution with 5 equiv of *n*-octynoyl-CoA (*20*) for 30 min at 4 °C. Excess inactivator was subsequently removed by ultrafiltration with a Centricon-10 filter. The apoprotein obtained in this manner had an undetectable level of activity. Subsequently, 1.2 equiv of 2′-deoxy-FAD was added, and the mixture was incubated at 4 °C overnight before ultrafiltration.

Characterization of Recombinant pMCAD and 2′-Deoxy-FAD pMCAD. Steady-state kinetic assays were performed in 50 mM potassium phosphate, pH 7.6, buffer at 25 °C using ferricenium as the electron shuttle and terminal electron acceptor (*21*). The concentration of the C_8-CoA substrate was varied from 0.2 to 200 μM. Enzyme concentrations were 1.3 nM for WT pMCAD and 100 nM for 2′-deoxy-FAD pMCAD. Initial velocities for the oxidation of C_8-CoA were measured by monitoring the decrease in the absorbance at 300 nm using a Cary-100 spectrometer (Varian). An extinction coefficient of 4300 M^{-1} cm^{-1} at 300 nm was used for the reduction of ferricenium ion. Kinetic parameters, k_{cat} and K_m, were determined by nonlinear least-squares fits of the initial velocity data to the Michaelis−Menten equation using Grafit 3.09b (Erithacus Software Ltd.).

Binding constants (K_d) of HD-CoA to the pMCAD and its mutants were measured spectrophotometrically by following the absorbance change of the bound FAD cofactor at 490 nm as a function of the HD-CoA concentration. K_d values were calculated using eq 1.

$$[ES] = (([E_o] + [S_o] + K_d) - (([E_o] + [S_o] + K_d)^2 - 4[E_o][S_o]))^{1/2}/2 \quad (1)$$

Raman Spectroscopy. Off-resonance Raman spectra were acquired as described previously using a 2 mm by 2 mm rectangular cell (*13*, *16*, *22*). Initially, 70 μL of oxidized enzyme (200−400 μM) was added to the cell, and 480 × 1 s scans were accumulated. Subsequently, the ligand (typically 1 or 2 μL of about 10 mM concentration) was introduced into the same cell and the sample mixed by careful stirring without changing the optical alignment or cell position. Following accumulation of a second spectrum (480 × 1 s) the Raman difference spectrum of the bound ligand was obtained by performing a computer subtraction of the spectrum of free enzyme from that of the corresponding enzyme−ligand complex. An appropriate scaling factor was applied to each subtraction to eliminate any residual protein signals. The difference spectra were wavenumber calibrated against cyclohexanone and are accurate to ±2 cm^{-1}. The software used to acquire Raman spectra was WinSpec (Princeton Instrument), and spectral manipulations were performed with Win-IR. The resolution of the Raman system is about 8 cm^{-1}.

Enzyme-Catalyzed α-Proton Exchange of C_8-CoA. The α-proton exchange of C_8-CoA catalyzed by recombinant

pMCAD, the E376Q mutant, and 2′-deoxy-FAD pMCAD was monitored by ^{1}H NMR spectroscopy at 25 °C. Prior to the NMR experiment, labile substrate protons were exchanged with deuterium by twice dissolving the substrate in D_2O followed by lyophilization. The concentration of the substrate was determined using an extinction coefficient of 16300 M^{-1} cm^{-1} at 260 nm. Enzymes were exchanged into 50 mM phosphate−D_2O buffer prepared by dissolving P_2O_5 in 99.7% D_2O and adjusting the pD to 7.6 (corresponding to a pH meter reading of 7.2) with anhydrous K_2CO_3. NMR samples consisted of 2 mM substrate and 2 μM enzyme in 0.5 mL of the D_2O−phosphate buffer. NMR spectra were recorded using either Varian Innova 500 or 600 MHz instruments in the SUNY Stony Brook NMR Center.

A typical exchange experiment started by taking the ^{1}H NMR spectrum of the pure substrate. Subsequently, an aliquot of the enzyme solution was added to the NMR tube to make the final enzyme concentration 2 μM, and the sample was mixed by inverting the tube twice. ^{1}H NMR spectra were recorded at various times after enzyme addition, and the integration of the α-proton resonance at 2.62 ppm was monitored. Sixteen scans were collected for each spectrum, and the NMR data were analyzed using Felix software, version 98 (Biosym, MSI).

Alterations in NMR peak integrals during the incubation of C_8-CoA with enzyme in D_2O buffer were analyzed using eq 2, where A_t is the integral at time t, A_i is the initial peak integral, A_f is the final peak integral, and k_{obs} is the observed first-order rate constant (*23*).

$$A_t = (A_i - A_f)e^{-k_{obs}t} + A_f \quad (2)$$

The exchange rate, k_{exc}, was calculated from eq 3, which takes into account the total amount of acyl-CoA bound at any time, where $[C_8\text{-CoA}]_T$ is the total acyl-CoA concentration and $[C_8\text{-CoA}]_B$ is the concentration of bound acyl-CoA. Since the concentration of C_8-CoA (2 mM) was significantly larger than the enzyme concentration (2 μM) and also the K_m for C_8-CoA (2.6 μM), the concentration of bound acyl-CoA ($[C_8\text{-CoA}]_B$) was equal to the enzyme concentration used.

$$k_{exc} = k_{obs}[C_8\text{-CoA}]_T/[C_8\text{-CoA}]_B \quad (3)$$

Spectroelectrochemistry. Electrochemical experiments were performed on MCAD from pig kidney. The pig kidneys were purchased from Lindenfelser Meats, Albertville, MN, and stored at −80 °C. MCAD purified as described by Lenn et al. (*4*) was >95% pure as determined by sodium dodecyl sulfate (SDS)−polyacrylamide gel electrophoresis. Spectrophotometric measurements were obtained using a Perkin-Elmer Lambda 12 spectrophotometer interfaced to a 486 computer and equipped with a thermostated cell compartment as well as a magnetic stirrer. Potentiometric and coulometric measurements were obtained using a BAS 50CV (BioAnalytical System) potentiostat interfaced with an PC computer running BAS system software. Data manipulation was performed with Perkin-Elmer system software, a standard spreadsheet program (Microsoft Excel), and a linear regression program (GraphPad Prizm 3.0). Anaerobic conditions needed for all redox experiments were obtained using an argon/vacuum system. The sample solution was placed in the airtight spectroelectrochemical cell and purged with argon followed immediately by a vacuum purge. All redox studies were at 25 °C in 50 mM potassium phosphate buffer, pH 7.6.

Table 1: Absorption Maxima of Free and Enzyme-Bound FAD

species	λ_{max} (nm)			ϵ (mM^{-1} cm^{-1})
FAD	266	374	445	11.3 (450 nm)[a]
pMCAD[b] (native)	270−275	370−373	445−447	15.4 (446 nm)[c]
pMCAD, WT (recombinant)	274	373	446	
pMCAD, E376Q	277	374	446	
pMCAD, E376P	275	376	448	
2′-deoxy-FAD pMCAD	274	376	441	

[a] Reference *42*. [b] References *43* and *17*. [c] Reference *17*.

In the potentiometric experiments, a small fraction of the enzyme and indicator dyes (pyocyanine and indigo disulfonate) were reduced by addition of reducing equivalents to establish an equilibrium defined as <1.0 mV/10 min drift. At the poised equilibrium, the potential of the system was measured via the potentiostat, and the optical spectrum was measured with the spectrophotometer. The procedure was repeated, generating absorption spectra with the system poised at the corresponding E, until the enzyme was completely reduced. Once corrected, the experimental enzyme spectra were analyzed using the Nernst equation:

$$E = E_m + 2.303\frac{RT}{nF}\log\left(\frac{[ACD_{ox}]}{[ACD_{red}]}\right) \quad (4)$$

where E is the measured potential at equilibrium of each point, E_m is the midpoint potential, R is the gas constant (8.314 J K^{-1} mol^{-1}), T is the temperature in kelvin, n is the number of electrons involved in the half-reaction, and F is the Faraday constant (96485 C mol^{-1}). The ratio of $[ACD_{ox}]/[ACD_{red}]$ for the enzyme was determined from these spectral data. In coulometric titrations, the enzyme was reduced by an electrochemically generated methyl viologen radical, and the absorption spectrum was collected. The procedure was repeated until the enzyme was fully reduced.

RESULTS

Absorption Spectra of the Recombinant pMCAD, E376Q, E376P, and 2′-Deoxy-FAD pMCAD. Recombinant pMCAD differs from the native enzyme by the addition of nine residues (QLEHHHHHH) at the C-terminus. Importantly, the UV−vis absorption spectrum of the WT recombinant enzyme was very similar to that of published data for the native enzyme, with an A_{280}/A_{446} ratio of 5.8 (Table 1). The absorption maxima of the recombinant and native enzymes as well as of the E376Q and E376P mutants were also very similar (Table 1), strongly suggesting that the recombinant enzymes were correctly folded. Consistent with Engst's observation (*11*), the UV−vis absorption spectrum of 2′-deoxy-FAD pMCAD was similar but not identical to that of the parent pMCAD. Specifically, the major absorption band of the reconstituted pMCAD in the visible region was blue shifted by 5 nm to 441 nm compared to that of the parent pMCAD at 446 nm (Table 1).

Table 2: Kinetic and Binding Constants for WT, Mutant, and 2′-Deoxy-FAD pMCAD[a]

enzyme	k_{cat} (s^{-1})	K_m (μM)	k_{cat}/K_m (μM^{-1} s^{-1})	K_d(HD-CoA) (μM)	k_{exc} (s^{-1})
native pMCAD[b]	19.6 ± 0.2	2.3 ± 0.1	8.5 ± 0.5	3.5[g]	
recombinant WT pMCAD[c]	18.8 ± 0.5	2.5 ± 0.4	7.5 ± 1.4	3.0	0.35 ± 0.03
FAD pMCAD[d]	20.0 ± 0.7	2.6 ± 0.5	7.7 ± 1.8		
2′-deoxy-FAD pMCAD[e]	0.047 ± 0.005	2.2 ± 0.3	0.021 ± 0.005	3.5	0.085 ± 0.005
recombinant hMCAD[b]	19.2 ± 0.3	3.0 ± 0.3	6.4 ± 0.7		
E376Q pMCAD[f]				3.4	
E376P pMCAD[f]				87	

[a] All parameters were measured at 25 °C. [b] Data taken from ref *29*. [c] Assayed with 1.3 nM enzyme concentration. [d] Pig MCAD reconstituted with commercial FAD. [e] Pig MCAD reconstituted with 2′-deoxy-FAD. [f] No activity detected using 100 nM enzyme. [g] Data taken from ref *13*.

Binding of HD-CoA to pMCAD. HD-CoA is a product analogue of MCAD that induces a change in the flavin absorption spectrum upon binding to the enzyme similar to that observed for other ligands (*3*, *6*, *24*−*28*). The binding constant (K_d) of HD-CoA toward native pMCAD was previously determined to be 3.5 μM (*13*). Using the same method, we determined a K_d value of 3.0 μM for HD-CoA binding to the recombinant WT pMCAD enzyme, again suggesting that the recombinant enzyme was correctly folded. Similar K_d values were observed for 2′-deoxy-FAD pMCAD (3.5 μM) and the E376Q mutant (3.4 μM). However, the K_d value for E376P (87 μM) was increased 29-fold compared to WT enzyme.

Steady-State Kinetics. The steady-state kinetic parameters obtained using C_8-CoA as substrate with the ferricenium assay (*21*) are summarized in Table 2. The k_{cat} value for recombinant WT pMCAD was 18.8 s^{-1} with a K_m of 2.5 μM. These kinetic parameters are close to the reported k_{cat} (19.6 s^{-1}) and K_m (2.3 μM) values for the native WT pMCAD enzyme (*29*), further supporting the notion that the recombinant and native enzymes are structurally and functionally identical.

The recombinant pMCAD reconstituted with 2′-deoxy-FAD showed a K_m (2.2 μM) similar to that of the WT pMCAD, indicating that the 2′-OH of the FAD cofactor is not essential in substrate binding. However, k_{cat} for the 2′-deoxy-FAD pMCAD was reduced 400-fold compared to WT enzyme with a value of 0.047 s^{-1}. As a control, the recombinant WT pMCAD was also reconstituted with normal FAD, and the activity was assayed in a parallel experiment. Importantly, the FAD-reconstituted pMCAD had kinetic parameters identical to those of the parent recombinant pMCAD enzyme (Table 2). Finally, both the E376Q and E376P mutants showed no detectable activity from the ferricenium assay under the same conditions as those of the WT pMCAD.

α-*Proton Exchange of C_8-CoA Catalyzed by pMCAD and 2′-Deoxy-FAD pMCAD*. Figure 1 contains the ^{1}H NMR spectrum of C_8-CoA in D_2O buffer between 1.4 and 2.8 ppm. Three signals are observed in this region of the spectrum, two triplets at 2.62 and 2.46 ppm, assigned to the octanoyl α-protons and the CoA 6″-methylene group, respectively, and a quintet at 1.61 ppm assigned to the octanoyl β-protons. Addition of WT pMCAD to the solution caused a progressive decrease in the integration of the α-proton resonance from two protons to one proton which was complete in 90 min. The decrease in intensity of the α-proton resonance results from the stereospecific exchange of one of the substrate's α-protons with solvent deuterium. The ^{1}H NMR spectrum

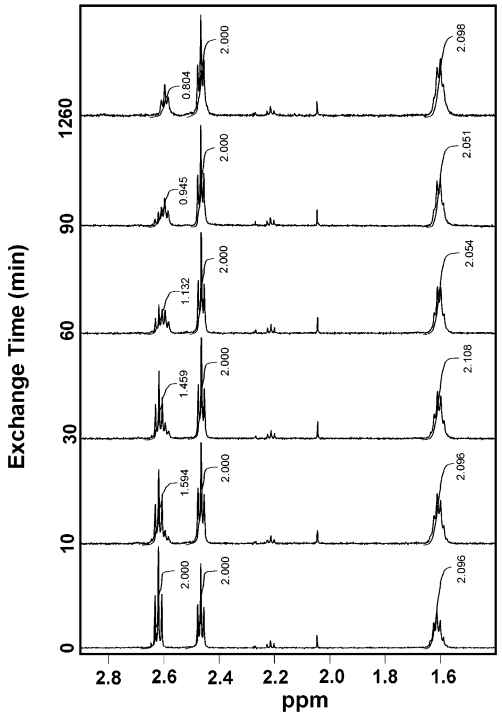

FIGURE 1: ^{1}H NMR spectra in the 1.4−2.8 ppm region of C_8-CoA (2 mM at time 0) and C_8-CoA incubated with 2 μM WT pMCAD at various times. Resonances in the spectrum acquired at time 0 are assigned to the octanoyl α-protons at 2.62 ppm, the CoA 6″-methylene group at 2.46 ppm, and the octanoyl β-protons at 1.61 ppm. Each spectrum was Fourier transformed from 16 scans. Data were processed and analyzed using Felix software, version 98 (Biosym, MSI). Spectra were referenced to the 11″-methyl-CoA resonance at 0.78 ppm (*18*). Integrals were normalized by setting the integral of the CoA 6″-methylene protons to 2.0.

of C_8-CoA isolated following the exchange reaction is shown in Figure 2 where it can be seen that the remaining α-proton resonance has shifted to 2.59 ppm. This 0.023 ppm upfield shift is in agreement with the normal geminal ^{2}H isotope effect. In addition, the quintet at 1.61 ppm assigned to the octanoyl β-proton resonance shifts to 1.60 ppm where it appears as a quartet upon completion of the exchange reaction. The alteration in the α-proton resonance with time is plotted in Figure 3 where the data have been analyzed using eq 2 to give a k_{obs} value of 0.021 min^{-1}. This k_{obs} value corresponds to an actual exchange rate (k_{exc}) of 0.35 s^{-1}, in agreement with previous studies using rat liver MCAD (*30*).

The ability of 2′-deoxy-FAD pMCAD to catalyze α-proton exchange was also analyzed. ^{1}H NMR spectra revealed that integration of the octanoyl α-proton resonance decreased from two protons to one proton over a period of 9 h (data not shown). Analysis of the exchange data as a function of

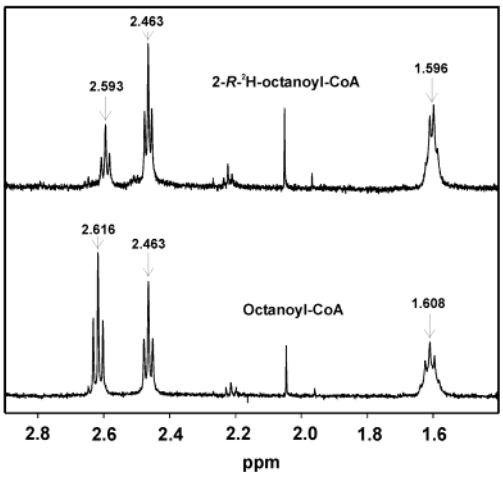

FIGURE 2: ^{1}H NMR spectra of C_8-CoA (2 mM, lower spectrum) and [2-(*R*)-^{2}H]octanoyl-CoA (2 mM, upper spectrum) shown in the aliphatic proton resonance region. Resonance assignments are given in the legend to Figure 1.

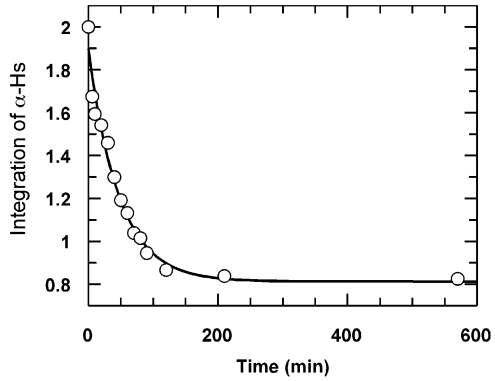

FIGURE 3: Plot of the α-proton resonance integral as a function of time following incubation of C_8-CoA with WT pMCAD. The solid line is a best fit to eq 2 with $k_{obs} = 0.021$ min^{-1}.

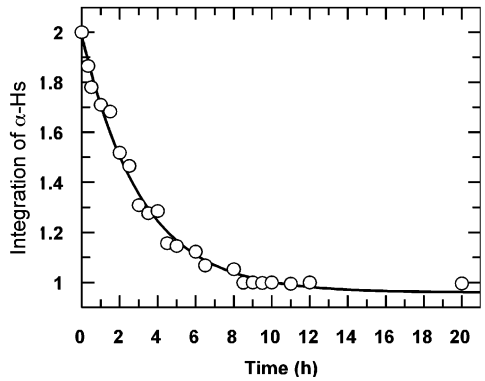

FIGURE 4: Plot of the α-proton resonance integral as a function of time following incubation of C_8-CoA with 2′-deoxy-FAD pMCAD. The solid line is a best fit to eq 2 with $k_{obs} = 0.31$ h^{-1}.

time (Figure 4) provided an observed exchange rate (k_{obs}) of 0.31 h^{-1}, corresponding to an actual exchange rate (k_{exc}) of 0.085 s^{-1}. Consequently, removal of the 2′-ribityl hydroxyl group results in a 4-fold decrease in exchange rate. Finally, in contrast to WT and 2′-deoxy-FAD enzymes, no α-proton exchange was observed when C_8-CoA was incubated with E376Q mutant for up to 48 h (data not shown), verifying the importance of E376 in the exchange process.

Raman Difference Spectra of HD-CoA Bound to 2′-Deoxy-FAD pMCAD and pMCAD Mutants. HD-CoA has been used extensively in the spectroscopic and electrochemical study of fatty acid oxidation enzymes (*13*, *14*, *31*). Previous Raman studies have shown that the dienoyl portion of HD-CoA is polarized in complexes with both the oxidized and reduced native pMCAD. This polarization is manifest by the replacement of a band at 1595 cm^{-1} in the spectrum of unbound HD-CoA with a band at 1568 cm^{-1} in the enzyme-bound complexes. While the 1595 cm^{-1} band in free HD-CoA arises from a vibrational mode delocalized over the entire HD skeleton, binding to the enzyme causes the terminal C4═C5 double bond to be vibrationally decoupled from the remainder of the molecule and results in the appearance of a new mode localized on the C3═C2─C1═O enone fragment at 1568 cm^{-1} (*13*, *31*).

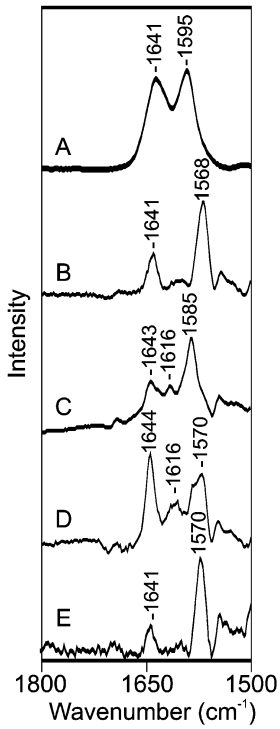

FIGURE 5: Raman difference spectra of HD-CoA (A) free in aqueous solution, (B) complexed with oxidized WT pMCAD, (C) complexed with 2′-deoxy-FAD pMCAD, (D) [$^{13}C_3$]-HD-CoA complexed with 2′-deoxy-FAD pMCAD, and (E) complexed with E376Q pMCAD. Enzyme concentrations were 380 μM for WT pMCAD, 360 μM for 2′-deoxy-FAD pMCAD, and 217 μM for E376Q pMCAD. In each case 0.8 equiv of HD-CoA was added to the enzyme samples.

The Raman spectrum of HD-CoA complexed to the recombinant WT pMCAD is similar to that of HD-CoA complexed to the native pMCAD (*13*). Upon binding to the recombinant wild-type enzyme, the vibrational band of the C3═C2─C1═O HD-CoA enone moiety was shifted to lower frequency by 27 cm^{-1} from 1595 to 1568 cm^{-1} (Figure 5A,B). For 2′-deoxy-FAD pMCAD, two predominant bands were observed at 1643 and 1585 cm^{-1} in the spectrum of HD-CoA bound to the enzyme (Figure 5C). The band at 1585 cm^{-1} was sensitive to isotope labeling of HD-CoA at the C3 (Figure 5D) and C1 positions (data not shown), identifying this band as a vibrational mode arising from the C3═C2─C1═O (enone fragment) of HD-CoA. The second band at 1643 cm^{-1} in spectrum C was insensitive to the two isotope labels and can be assigned to the terminal C4═C5 HD double bond. The weak band at 1616 cm^{-1} is also

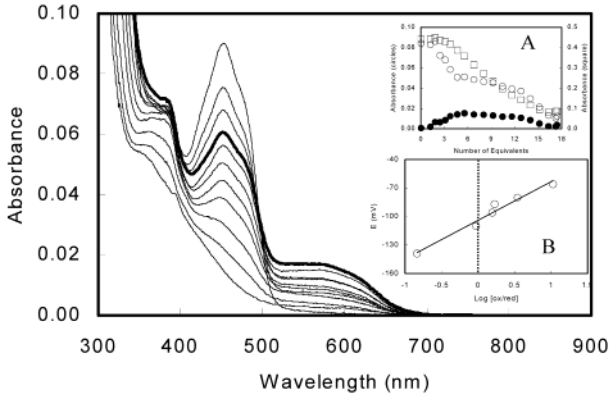

FIGURE 6: Coulometric titration of the HD-CoA−2′-deoxy-FAD pMCAD complex. The HD-CoA concentration was 46 μM while the 2′-deoxy-FAD pMCAD concentration was 6.1 μM, so the enzyme was 92% saturated. Titration was performed under anaerobic conditions in 50 mM potassium phosphate buffer, pH 7.6 at 25 °C. Inset A: Plot of absorbance at 308 nm (□), 455 nm (○), and 580 nm (●) as a function of the number of reducing equivalents (n) added during the titration. Inset B: Nernst plot giving an $E_m = -105$ mV and an $n = 1.5$ from a potentiometric titration of the HD-CoA−2′-deoxy-FAD pMCAD complex. The HD-CoA concentration was 55 μM, and the 2′-deoxy-FAD pMCAD concentration was 6.7 μM. Titration was performed under anaerobic conditions in 50 mM potassium phosphate buffer, pH 7.6 at 25 °C.

insensitive to isotope labeling of HD-CoA and was assigned to a flavin vibrational mode (*13*, *32*). Consequently, 2′-deoxy-FAD pMCAD induces only a 10 cm^{-1} decrease in the position of the HD enone band, from 1595 to 1585 cm^{-1}, in contrast to the 27 cm^{-1} change resulting from binding of HD-CoA to the wild-type enzyme. Lastly, Figure 5 also contains the Raman spectrum of HD-CoA bound to the E376Q pMCAD mutant (E) which is very similar to that obtained for the wild-type enzyme complex (B). This result indicates that, unlike 2′-deoxy-FAD MCAD, the E376Q mutant has retained the wild-type protein's ability to bind and polarize the ligand. Raman difference spectra were also obtained for HD-CoA in the presence of E376P (data not shown). However, the relatively weak binding of HD-CoA to this mutant ($K_d = 87$ μM) hindered detailed analysis of these data at the protein concentration used (344 μM).

Coulometric Titration of HD-CoA Bound to 2′-Deoxy-FAD-Reconstituted pMCAD. Coulometric and potentiometric studies were performed to investigate the effect of removing the ribose hydroxyl group on the redox properties of complexed and uncomplexed 2′-deoxy-FAD pMCAD. Coulometric titrations revealed that reduction of the complex results in loss of absorption at 455 nm (Figure 6). Analysis of the stoichiometry for the 2′-deoxy-FAD pMCAD−HD-CoA system indicates that two electrons are required for complete reduction of the enzyme. In addition, as the 455 nm absorbance decreases, the absorbance at 580 and 375 nm increases. This indicates that a mixture of red radical and blue neutral semiquinone (i.e., one-electron-reduced enzyme) is stabilized. The inset (A) of Figure 6 shows the spectral changes at selected wavelengths in order to monitor HD-CoA (308 nm), $pMCAD_{ox}$ (455 nm), and one-electron-reduced semiquinone ($pMCAD_{sq}$, 580 nm). It can be seen that $pMCAD_{ox}$ initially reduces to $pMCAD_{sq}$ until the maximum amount of semiquinone is formed (40%). As further equivalents are added to the system, both $pMCAD_{ox}$ and $pMCAD_{sq}$ are reduced to the two-electron-reduced hydroquinone ($pMCAD_{red}$). In addition, the HD-CoA absorbance also decreases during the entire titration, indicating that it is also accepting 2 equivalents of electrons. The overall titration required 17 reducing equivalents, which is in good agreement with the number of equivalents (*16*) required to reduce the enzyme (*2*) and the ligand (*14*) and the knowledge that 1 equivalent is initially consumed by molecular oxygen before reduction of the complex has started. This indicates that the enzyme and the ligand are coreducing, each accepting two electrons.

Table 3: Redox Potentials of HD-CoA−MCAD Complexes

	uncomplexed	native pMCAD	2′-deoxy-FAD pMCAD
none		−145[a]	−173,[b] −165[c]
hexadienoyl-CoA	−114	−52[d]	−115[e]

[a] Data taken from ref *26*. [b] Data taken from ref *12*. [c] Data taken from ref *11*. [d] Data taken from ref *13*. [e] Coreduced.

Potentiometric Titration of HD-CoA Bound to 2′-Deoxy-FAD-Reconstituted pMCAD. In agreement with the absorption data in Figure 6, the potentiometric titration revealed that the charge-transfer band found in the native complex between the reduced enzyme and HD-CoA is not present in 2′-deoxy-FAD pMCAD (data not shown). Because coreduction creates multiple species, the redox potential for the complex is more accurately described as a conditional midpoint potential ($\hat{E}_m$). The midpoint potential shifts from −171 to −115 mV upon complex formation (Figure 6, inset B). Consequently, the redox potential shift in the 2′-deoxy-FAD complex is +56 mV compared to +93 mV observed for the wild-type enzyme (Table 3). However, because this is a conditional midpoint potential, other factors (such as the ligand's redox potential or ligand protonation) may be contributing to the observed value. For example, the redox potential of HD-CoA itself may be exerting a considerable influence on the measured potential of the system. Consequently, the redox properties of HD-CoA were measured.

Redox Properties of Free HD-CoA. The redox potential of uncomplexed HD-CoA was also determined (data not shown). Because only the enzyme can transfer electrons between the dyes and the ligand, typical equilibration times were 4−5 h per point due to the low concentration of MCAD relative to HD-CoA. A Nernst plot was constructed, indicating that the redox potential for HD-CoA was −114 mV (Table 3). These data can be used to rationalize why unbound HD-CoA coreduces with the HD-CoA−2′-deoxy-FAD pMCAD complex (E_m −115 mV) since the redox potentials of both are very similar. In contrast, the redox potential of HD-CoA bound to WT pMCAD is −52 mV, and so in this case reduction of the complex is complete before the unbound HD-CoA starts to reduce.

DISCUSSION

Formation of the enzyme−substrate complex results in two important thermodynamic changes that enable MCAD to catalyze substrate oxidation. First, the pK_as of E376, the general base, and of the substrate's α-protons are matched in order to facilitate proton transfer (*3*, *6*). Second, upon binding the substrate, the redox potential of the FAD cofactor is raised over 110 mV to match that of the substrate (*26*). Subsequently, the reaction proceeds as concerted α-proton

Scheme 2

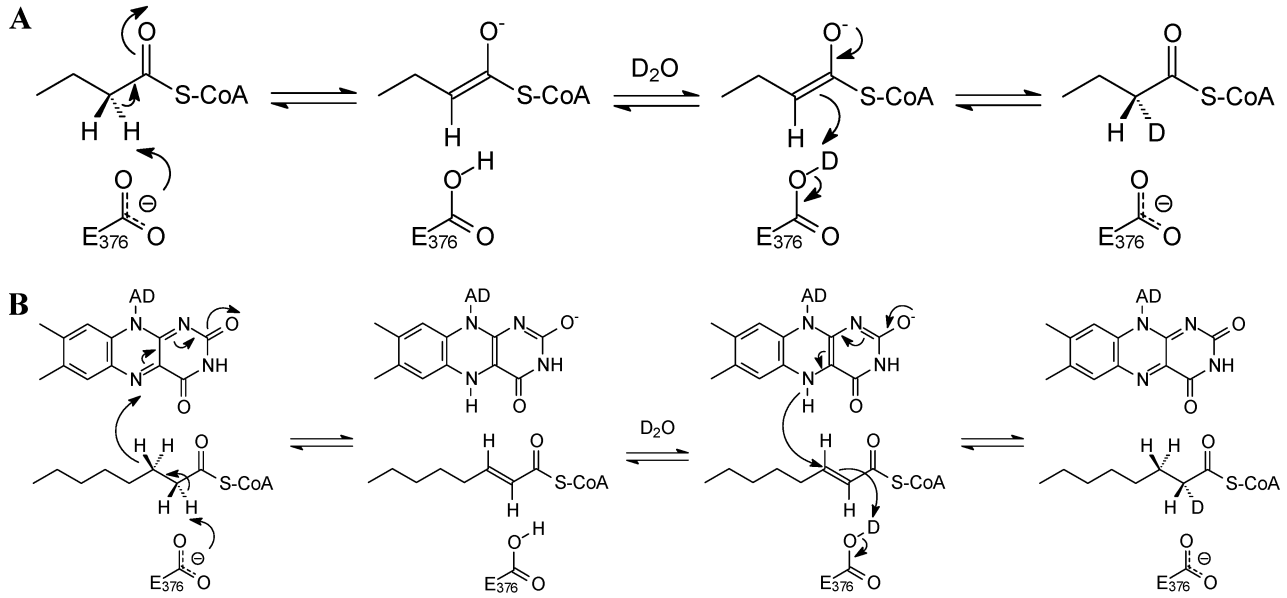

abstraction of the substrate by the carboxylate of E376 and β-hydride transfer to N5 of the FAD cofactor. While the increase in the pK_a of E376 to near neutral results from the displacement of five ordered water molecules in the active site of the protein by the substrate (*6*), the decrease in pK_a of the substrate's α-protons results from specific interactions between the enzyme and substrate in the active site. In the MCAD−C_8-CoA complex, the substrate carbonyl oxygen is hydrogen-bonded with the oxyanion hole comprising the ribityl 2′-hydroxyl of the FAD cofactor and the backbone amide of E376 (*8*). These hydrogen bonds are believed to play a key role in activating the substrate and stabilizing the transition state for substrate oxidation.

Evidence for the importance of the MCAD oxyanion hole has been inferred from data on substrate analogues that lack a carbonyl oxygen (*26*) and from data on MCAD reconstituted with 2′-deoxy-FAD (*11*, *12*). Ghisla, Kim, and co-workers reported that no catalytic activity was detected from 2′-deoxy-FAD MCAD using the ferricenium assay at an enzyme concentration of 30 nM (*11*). However, they did observe bleaching of the 2′-deoxy-FAD absorbance in the visible region upon incubation of 2′-deoxy-FAD MCAD with C_8-CoA and determined that the rate of flavin bleaching was 5.0×10^{-5} s^{-1} at 1 °C, indicating that there was dehydrogenation activity in the reconstituted enzyme. In addition, these workers observed that the pK_a of 3-thiaoctanoyl-CoA was only decreased by 5 pH units upon complexation with 2′-deoxy-FAD MCAD compared to 11 units with the wild-type enzyme. Finally, Bach and co-workers calculated the activation energy barriers for substrate oxidation using several MCAD active site models and concluded that the change in activation energy resulting from removal of the FAD 2′-hydroxy group was 10 kJ mol^{-1} and that the electron density resulting from abstraction of the substrate's α-proton was mainly localized on the thioester backbone (*33*).

In the present work, we have extended the above studies on the role of the oxyanion hole in MCAD catalysis using a combination of kinetics, Raman spectroscopy, and redox potential measurements. As many of the previous studies on MCAD had been performed with the porcine enzyme, we first undertook to recombinantly express this enzyme so that we could combine FAD reconstitution experiments with site-directed mutagenesis. Importantly, the k_{cat}, K_m, and k_{exc} values determined in this study for the recombinant WT pMCAD enzyme with C_8-CoA are similar to those reported previously for MCAD isolated from animal tissues (*21*, *29*, *30*). Removal of the FAD 2′-hydroxyl group resulted in a 400-fold reduction in k_{cat}, corresponding to an activation energy barrier increase of 15 kJ mol^{-1}. However, the K_m value of C_8-CoA for 2′-deoxy-FAD pMCAD was similar to that of the parent enzyme, indicating that the absence of 2′-hydroxyl group of the cofactor did not dramatically alter substrate binding. Since the oxyanion hole has been suggested to play a primary role in modulating the acidity of the substrate's α-protons, we undertook to determine whether the decrease in k_{cat} resulted from an increase in α-proton pK_a by determining the ability of 2′-deoxy-FAD pMCAD to catalyze α-proton exchange.

α-*Proton Exchange.* Exchange of the C_8-CoA α-proton(s) with solvent deuterium was monitored by ^{1}H NMR spectroscopy. Incubation of C_8-CoA with WT pMCAD in D_2O buffer resulted in a decrease in integration of the α-proton resonance with a rate constant (k_{exc}) of 0.35 s^{-1}, similar to the value reported previously for rat liver acyl-CoA dehydrogenase (*30*). In agreement with the previous studies by Ikeda (*30*), the NMR data support the stereospecific exchange of a single α-proton, presumably the *pro-2R* proton, with solvent deuterium. Two plausible mechanisms for α-proton exchange are shown in Scheme 2 in which the proton abstracted by E376 exchanges with solvent deuterium prior to reprotonation of the substrate. The critical role of E376 in this process is supported by the observation that the E376Q mutant is unable to catalyze α-proton exchange.

By analogy to the exchange reaction catalyzed by enoyl-CoA hydratase (*34*), the incorporation of solvent deuterium into C_8-CoA catalyzed by oxidized pMCAD could occur via the reversible formation of an enolate intermediate (Scheme 2A). In support of this proposal, Truhlar and co-workers recently revisited the interpretation of the kinetic isotope effect data with short-chain acyl-CoA dehydrogenase and

concluded that the reaction proceeded via the stepwise formation and breakdown of an enolate intermediate (*35*), rather than the concerted reaction involving the simultaneous removal of both hydrogens from the substrate (*36*, *37*). However, this mechanism for the exchange reaction must also account for the observation that oxidized MCAD and substrate can react to form reduced MCAD and product in the absence of an added electron acceptor (*37*). While there is no evidence in our NMR spectra for the accumulation of octenoyl-CoA in solution, the reversible oxidation of the substrate on the enzyme provides a mechanism for α-proton exchange regardless of whether the reaction is stepwise or concerted (Scheme 2B). In both mechanisms the proton abstracted by E376 must exchange with solvent while ligand is still bound to the enzyme, while in mechanism B the bound ligand must protect the proton on the FAD N5 from exchange.

Given that 2′-deoxy-FAD pMCAD catalyzes substrate oxidation 400-fold slower than the wild-type enzyme, we were surprised that removal of the 2′-hydroxyl group only reduced the rate of α-proton exchange ($k_{exc} = 0.085$ s^{-1}) by a factor of 4 compared to WT pMCAD. On the face of it, this suggests that removal of the hydrogen bond from the FAD 2′-hydroxyl group has had only a small effect on the acidity of the ligand's α-protons. However, comparison of the absolute exchange rates with the value of k_{cat} for substrate turnover is revealing. If the proton exchange mechanism(s) shown in Scheme 2 lie(s) on the reaction pathway, then the rate of proton abstraction and reprotonation catalyzed by E376 cannot be smaller than the k_{cat} value of around 20 s^{-1} determined for WT pMCAD. Thus, the rate-limiting step in the exchange process cannot be deprotonation/reprotonation of the substrate since the measured value of k_{exc} for WT pMCAD is only 0.35 s^{-1}. Instead, we propose that k_{exc} for WT pMCAD is the rate of exchange of E376 with solvent. This slow exchange of the protonated E376 residue in the enzyme−substrate complex is consistent with the proposal that the bound ligand completely protects the FAD N5−H from solvent exchange (*37*). Since proton abstraction must occur with a rate constant at least equal to the fastest step on the reaction pathway for substrate oxidation, then the acidity of the α-protons could have been reduced as much as 3800-fold by removal of the 2′-hydroxyl group if we assume that proton abstraction is now rate limiting for 2′-deoxy-FAD pMCAD (k_{exc} 0.085 s^{-1}) and given that Kumar and Srivastava have determined a rate constant (k_2) of 320 s^{-1} for the reduction of pMCAD by C_8-CoA (*38*). This limiting reduction in α-proton acidity is larger than the decrease in k_{cat} observed for 2′-deoxy-FAD pMCAD compared to WT pMCAD, and so the alteration in α-proton acidity caused by removal of the 2′-hydroxyl group could account for the reduced turnover rate for this enzyme.

The above arguments are based on the premise that the proton abstraction mechanism(s) shown in Scheme 2 lie(s) on the reaction pathway. However, it is also possible that the k_{exc} values are direct measurements of α-proton acidity and that the exchange reaction is orthogonal to substrate oxidation. In this case, removal of the 2′-hydroxyl group only causes a 4-fold reduction in α-proton acidity, equivalent to an increase in the activation energy barrier for proton exchange of only 3.4 kJ mol^{-1}. Since the latter value is significantly smaller than the increase in E_a of 15 kJ mol^{-1} for substrate oxidation caused by removal of the 2′-hydroxyl group, the reduction in k_{cat} observed for 2′-deoxy-FAD pMCAD cannot be ascribed to perturbation of the α-proton pK_a. It would then follow that the decrease in α-proton pK_a of at least 17 pH units that occurs on substrate binding cannot result from hydrogen bonding to the 2′-hydroxyl group. In support of this proposal, recent studies using enzyme reconstituted with 5-deaza-FAD have suggested that interaction between the flavin and the substrate plays a key role in α-proton acidity (*28*). Thorpe and co-workers determined that reduction of 5-deaza-FAD pMCAD was thermodynamically highly unfavorable, with an E_m of −240 mV compared to the E_m value of −145 mV for the normal enzyme. It was therefore expected that the 5-deaza-FAD enzyme would stabilize the enolate of an acyl-CoA. However, spectroscopic titrations showed that the ligand did not form a significant enolate species with the 5-deaza-FAD enzyme, and therefore it was concluded that not only was the deazaflavin incapable of accepting a hydride from the substrate but removal of the 5-nitrogen atom had also significantly perturbed the pK_a of the ligand's α-protons (*28*).

Returning to the exchange data with 2′-deoxy-FAD pMCAD, one final point can be made. For this enzyme, the k_{exc} value of 0.085 ± 0.005 s^{-1} is now numerically slightly larger (around 2-fold) than k_{cat} for substrate oxidation (0.047 ± 0.005 s^{-1}). If the difference in k_{exc} and k_{cat} is real, then a step following proton abstraction must be rate limiting. Since chemistry is presumably rate limiting for 2′-deoxy-FAD pMCAD, then in a stepwise mechanism the slow step would be hydride transfer from the substrate to the flavin. Alternatively, if these values are the same, then both k_{exc} and k_{cat} reflect the same rate-limiting step. This would be consistent with a concerted mechanism or a stepwise mechanism in which proton abstraction is partially rate limiting. A simple way to test these possibilities would be to determine whether deuteration at the substrate's C3 position affected the rate of α-proton exchange. If exchange at C2 occurs via a mechanism in which a hydride is reversibly transferred to the FAD N5 (Scheme 2B), then there should be an isotope effect on k_{exc} using [3-(*R*)-^{2}H]octanoyl-CoA. Of course, this will only illuminate whether the reaction catalyzed by 2′-deoxy-FAD pMCAD is stepwise or concerted. The situation in the wild-type enzyme may be different since removal of the 2′-hydroxyl group could have altered the mechanism.

While further experiments are required to differentiate between the possibilities described above, our preferred explanation for the exchange reaction catalyzed by pMCAD is that this process lies on the reaction pathway for substrate oxidation and occurs via the reversible interconversion of substrate and product on the enzyme. In the wild-type enzyme, k_{exc} reflects the rate-limiting exchange of the E_{376} COOH with solvent, while in 2′-deoxy-FAD pMCAD k_{exc} reflects a chemical step that occurs in substrate oxidation. Whether the reaction is stepwise or concerted is still apparently an open question.

Raman Spectroscopy. Previously, we reported that a vibrational band at 1595 cm^{-1} in the spectrum of free HD-CoA was replaced by a new band at 1568 cm^{-1} upon formation of the HD-CoA−pMCAD complex (*13*). On the basis of isotopic labeling and a detailed analysis of Raman data from complexes of HD-CoA and HD-oxyCoA bound to enoyl-CoA hydratase, we believe that the shift of this

enone vibrational band to lower frequency results from an alteration of vibrational coupling within the HD skeleton caused largely by a reduction in bond order of the HD carbonyl group (*13*, *31*). Provided that the perturbation in the vibrational spectrum arises solely from hydrogen bonding to the HD carbonyl, our extensive studies on enoyl-CoA hydratase enable us to estimate a hydrogen bond enthalpy of 27 kJ mol^{-1} for the interaction of the HD carbonyl group with the enzyme's oxyanion hole (*14*, *31*). On the basis of arguments previously put forth on the enoyl-CoA hydratase system, we believe that the observed ligand polarization stems from catalytically relevant stress on the ligand which is a consequence of placing the ligand in an environment that is complementary to the transition state for the reaction rather than the ground state (*31*, *39*). Consequently, up to 27 kJ mol^{-1} may be available in ground state destabilization for catalyzing substrate oxidation (*31*). Furthermore, the electron redistribution that occurs upon ligand binding would be expected to acidify the C_α of the substrate due to the increase in electron density at this carbon, thereby lowering the pK_a of the α-proton. Finally, the redistribution of electron density resulting from the observed polarization would also be expected to favor hydride transfer from the C_β position, since accumulation of positive charge on this carbon would favor elimination of a hydride from the substrate.

The loss of partial catalytic ability of pMCAD upon reconstitution with 2′-deoxy-FAD is in agreement with data from Raman spectroscopy. In Figure 5 it can be seen that removal of the 2′-hydroxyl group results in a decrease in the HD enone band of only 10 cm^{-1}, from 1595 to 1585 cm^{-1}, as compared to a shift of 27 cm^{-1} for the wild-type enzyme. On the basis of Raman studies of HD-CoA bound to the related enzyme enoyl-CoA hydratase (see above) (*14*), we estimate that removal of the 2′-hydroxyl group has resulted in a 17 kJ mol^{-1} decrease in hydrogen bond enthalpy between the HD carbonyl group and pMCAD. This analysis assumes a linear correlation between hydrogen bond enthalpy and enone band position, an assumption that is supported by experimental hydrogen-bonding studies with model α,β-unsaturated esters and thioesters (*40*, *41*). In addition, we have used ab initio calculations to explore the relationship between hydrogen bond distance and wavenumber of the enone band in HD-CoA (data not shown). Using methanol as the hydrogen bond donor and altering the hydrogen bond distance (O−O) from 2.7 to 3.2 Å, we calculate a linear dependence between hydrogen bond distance and enone band position. Interestingly, the decrease in hydrogen bond enthalpy upon removal of the 2′-hydroxyl group is quantitatively similar to the 15 kJ mol^{-1} increase in activation energy for substrate turnover, calculated from the 400-fold decrease in k_{cat} for 2′-deoxy-FAD pMCAD. Thus, we believe that ligand polarization and reactivity, both stemming from hydrogen bonding in the oxyanion hole, are intimately linked.

Redox Potential Measurements. Spectroelectrochemistry reveals that the redox potential shifts caused by the binding of HD-CoA to the enzyme are +93 and +58 mV for the native pMCAD and 2′-deoxy-FAD pMCAD complexes, respectively (Table 3). These potential shifts correspond to free energy perturbations of −18 and −11 kJ mol^{-1} for the native and 2′-deoxy complexes, respectively. Consequently, assuming that HD-CoA is a true product analogue (*13*), removal of the 2′-hydroxy group has made substrate oxidation less favorable by 7 kJ mol^{-1}, or the ability of the ligand to activate the enzyme for substrate oxidation has been decreased by about 40%. The alteration in redox potential may be compared with the changes in activation energy inferred from the Raman data, where the hydrogen bond enthalpy between enzyme and ligand has been reduced from a maximum value of 27 kJ mol^{-1} to 10 kJ mol^{-1} by removal of the 2′-hydroxy group. The difference in hydrogen bond enthalpy of 17 kJ mol^{-1} calculated from the ability of the enzyme to cause ligand polarization is somewhat larger than the 7 kJ mol^{-1} decrease in redox potential for the system but is close to the increase in activation energy of 15 kJ mol^{-1} calculated from k_{cat}. Thus, while removal of the 2′-hydroxy group causes changes in ligand activation that can be directly correlated with the decrease in substrate turnover, changes in redox potential induced by ligand binding must arise from other factor(s) such as desolvation of the active site in addition to ligand polarization arising from hydrogen bonding in the oxyanion hole.

ACKNOWLEDGMENT

We are grateful to Dr. Hiroshi Yasue at the National Institute of Agricultural Resources, Japan, for providing the pMCAD cDNA. We are also grateful to Dr. Hung-wen (Ben) Liu for the 2′-deoxy-FAD for the initial studies.

REFERENCES

1. Beinert, H. (1963) in *The Enzymes* (Boyer, P. D., Lardy, H., and Myrback, K., Eds.) pp 447−466, Academic Press, New York.
2. Thorpe, C., and Kim, J. J. (1995) *FASEB J. 9*, 718−725.
3. Trievel, R. C., Wang, R., Anderson, V. E., and Thorpe, C. (1995) *Biochemistry 34*, 8597−8605.
4. Lenn, N. D., Stankovich, M. T., and Liu, H. W. (1990) *Biochemistry 29*, 3709−3715.
5. Ghisla, S., Braunwarth, A., and Vock, P. (1997) in *Flavins and Flavoproteins* 1996 (Stevenson, K. J., Massey, V., and Williams, C. H. J., Eds.) pp 629−632, University of Calgary Press, Calgary, Alberta, Canada.
6. Vock, P., Engst, S., Eder, M., and Ghisla, S. (1998) *Biochemistry 37*, 1848−1860.
7. Rudik, I., Ghisla, S., and Thorpe, C. (1998) *Biochemistry 37*, 8437−8445.
8. Kim, J. J. P., Wang, M., and Paschke, R. (1993) *Proc. Natl. Acad. Sci. U.S.A. 90*, 7523−7527.
9. Matthews, D. A., Alden, R. A., Birktoft, J. J., Freer, S. T., and Kraut, J. (1975) *J. Biol. Chem. 250*, 7120−7126.
10. Nishina, Y., Sato, K., Hazekawa, I., and Shiga, K. (1995) *J. Biochem. 117*, 800−808.
11. Engst, S., Vock, P., Wang, M., Kim, J. J. P., and Ghisla, S. (1999) *Biochemistry 38*, 257−267.
12. Johnson, B. D., Mancini-Samuelson, G. J., and Stankovich, M. T. (1995) *Biochemistry 34*, 7047−7055.
13. Pellet, J. D., Sabaj, K. M., Stephens, A. W., Bell, A. F., Wu, J., Tonge, P. J., and Stankovich, M. T. (2000) *Biochemistry 39*, 13982−13992.
14. Bell, A. F., Wu, J., Feng, Y., and Tonge, P. J. (2001) *Biochemistry 40*, 1725−1733.
15. Rabin, R., Megraw, R. E., Reeves, H. C., and Aji, S. J. (1965) *Life Sci. 4*, 1233−1239.
16. Rudik, I., Bell, A. F., Tonge, P. J., and Thorpe, C. (2000) *Biochemistry 39*, 92−101.
17. Thorpe, C., Matthews, R. G., and Williams, C. H. J. (1979) *Biochemistry 18*, 331−337.
18. Wu, W. J., Anderson, V. E., Raleigh, D. P., and Tonge, P. J. (1997) *Biochemistry 36*, 2211−2220.
19. Mayer, E. H., and Thorpe, C. (1981) *Anal. Biochem. 116*, 227−229.
20. Freund, K., Mizzer, J., Dick, W., and Thorpe, C. (1985) *Biochemistry 24*, 5996−6002.

21. Lehman, T. C., Hale, D. E., Bhala, A., and Thorpe, C. (1990) *Anal. Biochem. 186*, 280−284.
22. Bell, A. F., He, X., Wachter, R. M., and Tonge, P. J. (2000) *Biochemistry 39*, 4423−4431.
23. D'Ordine, R. L., Bahnson, B. J., Tonge, P. J., and Anderson, V. E. (1994) *Biochemistry 33*, 14733−14742.
24. Lau, S. M., Brantley, R. K., and Thorpe, C. (1988) *Biochemistry 27*, 5089−5095.
25. Johnson, J. K., Wang, Z. X., and Srivastava, D. K. (1992) *Biochemistry 31*, 10564−10575.
26. Johnson, B. D., and Stankovich, M. T. (1993) *Biochemistry 32*, 10779−10785.
27. Pace, C. P., and Stankovich, M. T. (1994) *Arch. Biochem. Biophys. 313*, 261−266.
28. Rudik, I., and Thorpe, C. (2001) *Arch. Biochem. Biophys. 392*, 341−348.
29. Peterson, K. L., Sergienko, E. E., Wu, Y., Kumar, N. R., Strauss, A. W., Oleson, A. E., Muhonen, W. W., Shabb, J. B., and Srivastava, D. K. (1995) *Biochemistry 34*, 14942−14953.
30. Ikeda, Y., Hine, D. G., Okamura-Ikeda, K., and Tanaka, K. (1985) *J. Biol. Chem. 260*, 1326−1337.
31. Bell, A. F., Feng, Y., Hofstein, H. A., Parikh, S., Wu, J., Rudolph, M. J., Kisker, C., Whitty, A., and Tonge, P. J. (2002) *Chem. Biol. 9*, 1247−1255.
32. Nishina, Y., Sato, K., Shiga, K., Fujii, S., Kuroda, K., and Miura, R. (1992) *J. Biochem. 111*, 699−706.
33. Bach, R. D., Thorpe, C., and Dmitrenko, O. (2002) *J. Phys. Chem. B 106*, 4325−4335.
34. Feng, Y., Hofstein, H. A., Zwahlen, J., and Tonge, P. J. (2002) *Biochemistry 41*, 12883−12890.
35. Poulsen, T. D., Garcia-Viloca, M., Gao, J., and Truhlar, D. G. (2003) *J. Phys. Chem.* (in press).
36. Pohl, B., Raichle, T., and Ghisla, S. (1986) *Eur. J. Biochem. 160*, 109−115.
37. Schopfer, L. M., Massey, V., Ghisla, S., and Thorpe, C. (1988) *Biochemistry 27*, 6599−6611.
38. Kumar, N. R., and Srivastava, D. K. (1994) *Biochemistry 33*, 8833−8841.
39. Cheng, H., Nikolic-Hughes, I., Wang, J. H., Deng, H., O'Brien, P. J., Wu, L., Zhang, Z. Y., Herschlag, D., and Callender, R. (2002) *J. Am. Chem. Soc. 124*, 11295−11306.
40. Tonge, P. J., Fausto, R., and Carey, P. R. (1996) *J. Mol. Struct. 379*, 135−142.
41. Clarkson, J., Tonge, P. J., Taylor, K. L., Dunaway-Mariano, D., and Carey, P. R. (1997) *Biochemistry 36*, 10192−10199.
42. Benecky, M., Li, T. Y., Schmidt, J., Frerman, F., Watters, K. L., and McFarland, J. (1979) *Biochemistry 18*, 3471−3476.
43. Hall, C. L., and Kamin, H. (1975) *J. Biol. Chem. 250*, 3476−3486.

BI0344578